Bull. Mater. Sci. (2019) 42:148
https://doi.org/10.1007/s12034-019-1830-4

Synthesis of CdSe and CdSe:Ga nanostructures for antibacterial application

WISAM J AZIZ
Faculty of Science, Physics Department, Mustansiriyah University, Baghdad 00964, Iraq
wisamj.aziz@uomusttansiriyah.edu.iq

MS received 17 June 2018; accepted 15 December 2018; published online 13 May 2019

Abstract. In this paper, the preparation of CdSe and CdSe:Ga nanoparticles using two methods: thermal evaporation and pulse laser ablation has been reported. Their structural properties were characterized using X-ray diffraction (XRD) and field emission scanning electron microscopy (FESEM). As confirmed by the XRD curves, CdSe and CdSe:Ga nanoparticles exhibited polycrystalline and wurtzite hexagonal structures with orientation planes of (100), (101), (102), (110) and (112). Also, a homogeneous distribution of nano-rod, flower-like, cylindrical, hexagonal and both nano-rod and hexagonal shapes with different diameters was seen by FESEM images. The band gaps of CdSe and CdSe:Ga (without annealed and annealed at temperatures of 150 (6 h) and 500°C (1 h)) were found to be 1.72, 1.7, 1.69 and 1.64 eV, respectively. The antibacterial activity could be increased by annealing CdSe:Ga nanoparticles at 150°C for 6 h in Gram-positive bacteria (*Bacillus subtilis*), whereas it is decreased in Gram-negative bacteria (*Enterobacter cloacae*). Alternatively, annealing CdSe:Ga at 500°C for 1 h led to an increase in the antibacterial activity in both Gram-positive and Gram-negative bacteria. It is concluded that the antibacterial activity is highly dependent on the type of bacteria, material, preparation conditions and the used methods.

Keywords. Cdse; Ga-doped; nanoparticles; PLA; antibacterial activity.

1. Introduction

Laser ablation is a typical example of the top-down approach of nanoparticle fabrication [1]. Nanoparticles have great scientific interest as they are effectively a bridge between bulk materials and atomic or molecular structures; physical, chemical and biological properties of substances are different from those exhibited by the micro-scale or bulk materials [2]. With benefiting new properties, it is expected to open various routes for the development of semiconductor materials, devices and systems that are superior to those in use today, and is advantageous in laser ablation in liquids and chemical etching, due to the smaller size of nanoparticles [3]. The concept of the bottom-up approach is that one may start with atoms or molecules so that larger structures are possibly built up such as the thermal evaporation technique [4,5]. Recently, for instance, CdSe could result in different nanostructures, such as nano-belts, nano-ribbons, nano-wires, nano-tubes, nano-sheets, nano-rods and nanoparticles (cadmium telluride (CdTe) and Ag, Ga, Cu) and its antimicrobial activities have been reported against both Gram-positive and Gram-negative bacteria [6–10].

The oxidative stress that occurred in the bacteria cell is induced by reactive oxygen species (ROS) which generated nanoparticles (NP materials yielded more ROS than bulk materials due to larger surface areas of NPs) to be the main mechanism of their antibacterial activity and swell the cell membranes of bacteria and destroys them. Furthermore, the heavy ions like Cd, Se and Ga NPs generated three types of ROS (superoxide radical, hydroxyl radical and singlet oxygen). The general principle occurs when illuminated the heavy ions by incident light with photon energy greater than the band gap, the electrons and the holes will be generated in NP materials. Electrons in the conduction band (CB) and holes in the valence band exhibit high reducing and oxidizing powers, respectively. The electrons can be reacted with molecular oxygen to produce a superoxide anion (O_2^-), while the holes will generate the hydroxyl radicals (OH) from an oxidative process. O_2^- and OH can damage virtually all types of organic biomolecules; including nucleic acids, carbohydrates, proteins, DNA and amino acids, as a result they can destroy the most kinds of bacteria [11].

2. Experimental

CdSe and CdSe:Ga (2%) samples were prepared by directly mixing high purity Cd (99.99) powder with a ratio of 58.66% and Se powder of purity (99.99) with a ratio of 41.34% according to the atomic ratios of their constituent elements. The mixture of CdSe was placed in evacuated quartz ampoules under a pressure of 10^{-3} torr. The ampoules were placed inside the furnace at 1100°C for 5 h according to the phase diagram of the CdSe alloy at a constant thermal rate of 7°C min^{-1}. During the thermal process, the ampoule was constantly rocked to obtain a homogeneous mixture of the alloys.

The ampoules were broken, and then the compound was taken out to be milled into powder. The powder was used as a source of the pellet which was used as a target for pulse laser ablation (PLA). The CdSe target was immersed in *N*,*N*-dimethylformamide (DMF) solvent and fixed at bottom of the glass vessel container. The Nd:YAG laser system (HUAFEI type) provides pulses of a wavelength of 1064 nm and was used for ablating the CdSe target with an energy per pulse frequency of 800 mJ, pulse duration of 10 ns, repetition rate of 1 Hz and effective beam diameter of 4.8 mm.

The number of laser pulses was 2000. With the ablation of the CdSe target in distilled water, colloidal CdSe nanoparticles were formed. To make solution homogeneity, the colloidal was dispersed ultrasonically for 15 min and stirred with magnetic stirrer for 30 min. Thereafter, the solution was drop casted on a clean glass and it was placed on a hotplate stirrer at a temperature of 90°C for 20 min. Subsequently, a Ga plate of 99.99% purity was used as the target under the same conditions of PLA and the colloidal product was the volumetric mixture with the CdSe (98%) and Ga (2%) ratio. The CdSe:Ga samples were thermally treated at temperatures of 150°C for 6 h and at 500°C for 1 h. The thickness of the deposited materials was calculated as 120 ± 10 nm using the weight method. CdSe and CdSe:Ga nanoparticles were characterized using X-ray diffraction (XRD), field emission scanning electron microscopy (FESEM), and ultra–violet visible (UV–Vis) measurements.

3. Structural properties of CdSe and CdSe:Ga nanoparticles

3.1 *XRDL*

The crystal structure and orientation of CdSe and CdSe:Ga nanoparticles were investigated using XRD. Figure 1 shows the XRD curves of CdSe and CdSe:Ga nanoparticles in which polycrystalline and hexagonal wurtzite structures are clearly seen. The values are highly oriented with (100), (101), (102), (110) and (112) planes and are presented in table 1.

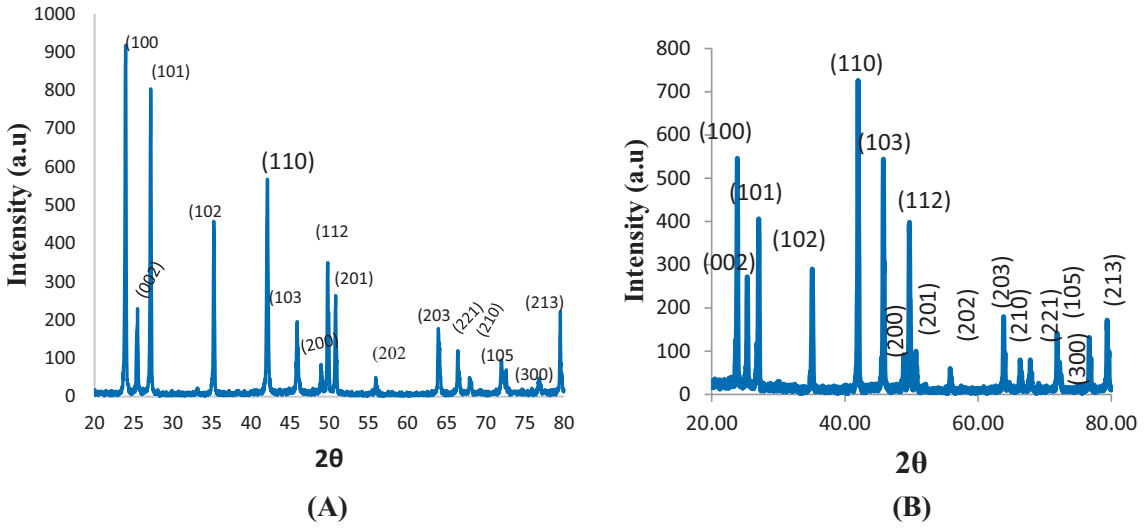

Figure 1. XRD patterns of (**A**) CdSe nanoparticles and (**B**) CdSe and CdSe:Ga nanoparticles.

Table 1. Comparing XRD of CdSe and CdSe:Ga prepared with the ASTM card.

CdSe			CdSe:Ga		
(*hkl*)	2θ (ASTM)	2θ prepared	(*hkl*)	2θ (ASTM)	2θ prepared
(100)	23.90	23.71	(202)	55.84	55.97
(002)	25.35	25.48	(203)	63.88	63.96
(101)	27.08	27.20	(210)	66.38	66.44
(102)	35.10	35.27	(211)	67.85	67.98
(110)	41.96	42.09	(105)	71.90	72.01
(103)	45.78	45.90	(212)	72.29	72.42
(200)	48.84	48.98	(300)	76.72	76.80
(112)	49.66	49.81	(213)	79.430	79.54
(201)	50.81	50.81			

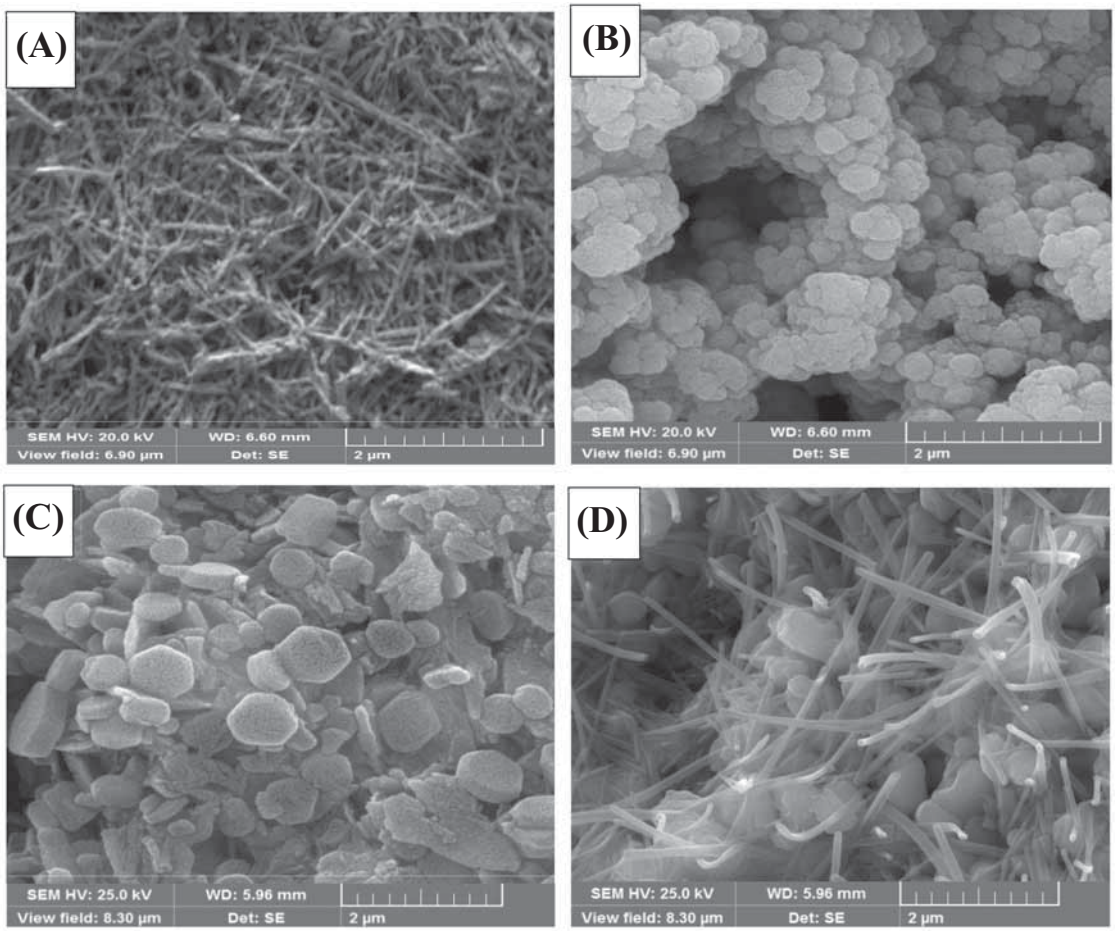

Figure 2. FESEM images of CdSe and CdSe:Ga thin films (**A**) CdSe, (**B**) CdSe:Ga, (**C**) annealing of CdSe:Ga at 150°C for 6 h and (**D**) annealing of CdSe:Ga at 500°C for 1 h.

The crystal size (D) was calculated based on the width of the preferring plane (002) by using Scherrer's formula [12]:

$$D = \frac{K\lambda}{\beta \cos\theta}, \tag{1}$$

where, k is the constant ($k = 0.9$), λ the wavelength of X-ray, β the full-width at half maximum of the diffraction peak and θ the Bragg's angle. The crystallite size of CdSe nanoparticles is around 30 nm and it changes to 27 nm upon the addition of Ga metal to form CdSe:Ga nanoparticles.

3.2 *FESEM*

Figure 2 shows the formation of CdSe and CdSe:Ga prepared by PLA using DMF as the surfactant agent. The image (figure 2A) of CdSe shows the formation of a homogeneously distributed nano-rod shape with a diameter of 5–10 nm. The image (figure 2B) of CdSe:Ga shows the formation of a flower-like shape with a diameter of 50–100 nm without any annealing temperature. The image (figure 2C) shows the effect of annealing temperature at 150°C for 6 h on CdSe:Ga nanoparticles, illustrating the formation of a hexagonal shape. The nano-crystals have a cylindrical shape with a diameter of about 300 nm. Furthermore, as figure 2D shows, when the annealing temperature was increased to 500°C for 1 h, CdSe:Ga nanoparticles show the formation of small amounts of randomly distributed nano-rods with the hexagonal nano-crystals with a diameter of 250 nm.

3.3 *Optical properties*

3.3a *Absorption*: As shown in figure 3, the absorption spectra of CdSe and CdSe:Ga nanoparticles increase with thermal treatment at 150°C for 6 h and 500°C for 1 h which result in re-ordering of crystallites inside the material. The Ga doping and thermal treatment processes are accompanied by a red shift of the absorption edge.

3.3b *Optical energy gap*: The band gaps of CdSe and CdSe:Ga at low and high annealing temperatures are shown in figure 4 and table 2. The electrical conductivity increases

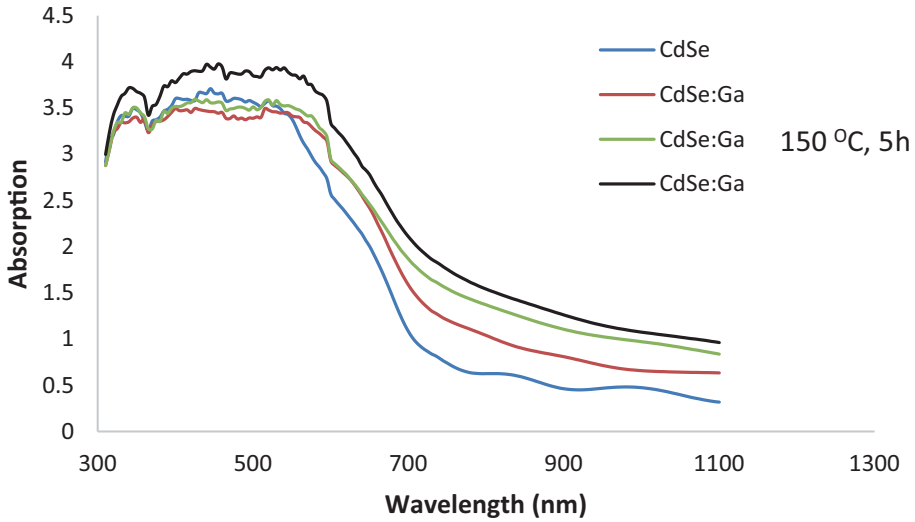

Figure 3. Optical absorption of CdSe and CdSe:Ga with different heat treatments.

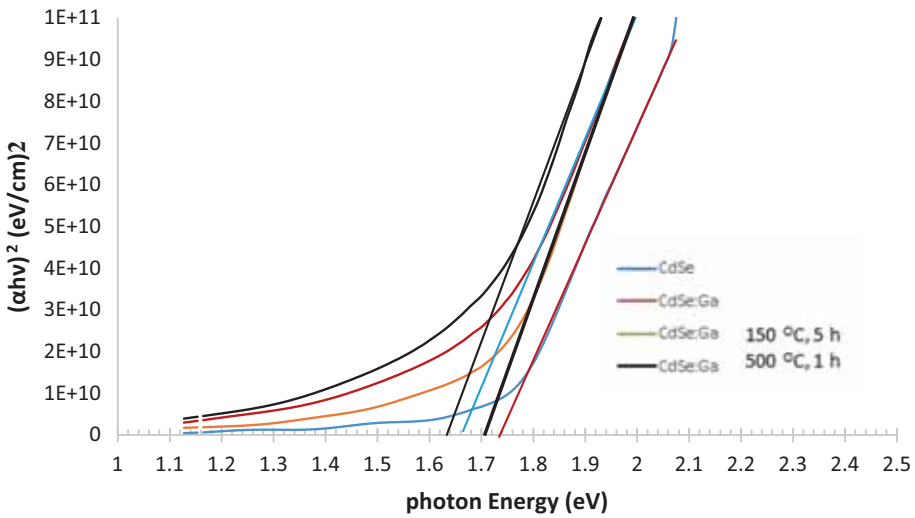

Figure 4. Optical band gap energy of CdSe and CdSe:Ga at different annealing temperatures.

Table 2. Summary of the optical energy gap of CdSe and CdSe:Ga with different heat treatments.

Materials	Band gap (eV)
CdSe pure	1.72
CdSe:Ga	1.70
CdSe:Ga with 150°C for 6 h	1.69
CdSe:Ga with 500°C for 1 h	1.64

with the addition of doped gallium, because the atoms of gallium led to induce the donor levels within the energy gap near the CB and this led to stimulate a larger number of electrons with small energies, which results in a decrease in the energy gap, this result is in accordance with other research studies [13–15]. Also obviously, the direct band gaps of CdSe:Ga nanoparticles were reduced with the increase in annealing temperature.

3.4 *Antibacterial studies*

The antibacterial studies of CdSe and CdSe:Ga nanostructures were tested against two standard bacterial isolates: Gram-positive bacteria (*Bacillus subtilis*) and Gram-negative bacteria (*Enterobacter cloacae*). The antibacterial activity of the compound against micro-organisms depends on the cell wall (membrane). In nature, sometimes the bacteria are exposed to extreme environmental conditions. To survive from these hard conditions, ultimately the bacteria depend on their ability to resist the effects of difficult environments.

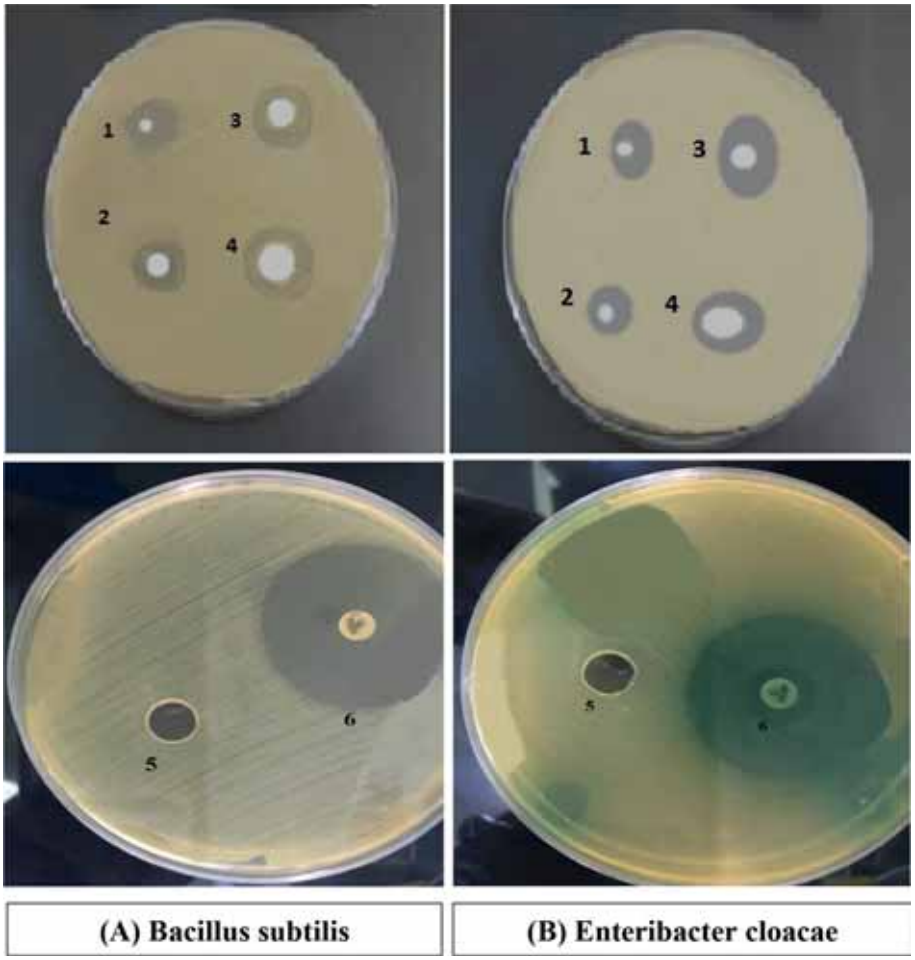

Figure 5. Antibacterial activity of (1) CdSe, (2) CdSe:Ga, (3) CdSe:Ga annealing at 150°C for 6 h, (4) CdSe:Ga annealing at 500°C for 1 h, (5) distilled water (no treatment) and (6) antibacterial agent (Meropenem). (**A**) *B. subtilis* and (**B**) *E. cloacae*.

Table 3. Antibacterial activity of CdSe and CdSe:Ga against: *B. subtilis* and *E. cloacae*.

Materials	The inhibition diameter zones (mm)	
	Gram-positive bacteria (*B. subtilis*)	Gram-negative bacteria (*E. cloacae*)
CdSe	10	11
CdSe:Ga	14	12
CdSe:Ga (150°C/6 h)	15	14
CdSe:Ga (500°C/1 h)	17	16
Distilled water	—	—
Meropenem	20	19

The bacteria have natural defence to deal with a variety of stresses such as toxicity [16].

Figure 5 shows the inhibition zone of CdSe, CdSe:Ga and CdSe:Ga annealed at 150°C for 6 h and CdSe:Ga annealed at 500°C for 1 h. As listed in table 3, the CdSe solution shows some activity against *B. subtilis* and *E. cloacae*. On the other hand, the antibacterial activity of CdSe:Ga was found to be increased in comparison with the pure CdSe. Moreover, the antibacterial activity of CdSe:Ga nanostructures annealed at 150°C for 6 h in Gram-positive bacteria (*B. subtilis*) increases, whereas the activity decreases in Gram-negative bacteria (*E. cloacae*)

because the Gram-negative bacteria are more resistant than the Gram-positive bacteria against their antibodies due to their impenetrable cell walls. Finally, CdSe:Ga annealing at 500°C for 1 h will show an increase in activity in both Gram-positive and Gram-negative bacteria. It is inferred that the antibacterial activity depends on the type of bacteria, materials and preparation conditions.

4. Conclusions

The synthesis of CdSe and CdSe:Ga nanoparticles using two methods: thermal evaporation and PLA has been demonstrated. The XRD results of CdSe and CdSe:Ga nanoparticles showed polycrystalline and hexagonal wurtzite structures. SEM images of CdSe revealed the formation of homogenously distributed with nano-rod shape and a diameter of 5–10 nm. Furthermore, the CdSe:Ga image showed the formation of a flower-like shape with a diameter of 50–100 nm without any annealing temperature. The effect of annealing temperature at 150°C for 6 h on CdSe:Ga nanoparticles illustrated the formation of a hexagonal shape with a diameter of about 300 nm. When the annealing temperature was increased to 500°C for 1 h, the CdSe:Ga nanoparticles showed the formation of randomly distributed nano-rods with hexagonal nano-crystals with a diameter of 250 nm. The band gaps of CdSe and CdSe:Ga at low and high annealing temperatures obtained a direct band gap and are reduced with the increase in annealing temperature. CdSe solution showed some activity against *B. subtilis* and *E. cloacae*. On the other hand, the antibacterial activity of CdSe:Ga was found to be increased in comparison with the pure CdSe. Moreover, the antibacterial activity of the annealed CdSe:Ga nanostructures at 150°C for 6 h in Gram-positive bacteria (*B. subtilis*) increased, whereas the activity decreased in Gram-negative bacteria (*E. cloacae*). Finally, CdSe:Ga annealing at 500°C for 1 h showed an increase in activity in both Gram-positive and Gram-negative bacteria. It is inferred that the antibacterial activity depends on the type of bacteria, materials and preparation conditions.

References

[1] Qinghu Y, Hua C, Kun G, Zhigao H, Shuang G, Peipei L, Jian S *et al* 2015 *J. Alloys Compd.* **626** 415
[2] Kim T W, Lee D U, Choo D C, Kim J H, Jeong J H, Jung M *et al* 2002 *J. Phys. Chem. Solids* **63** 881
[3] Gondal M A, Drmosh Q A, Yamani Z H and Rashid M 2009 *Int. J. Nanoparticles* **2** 119
[4] Pal J and Chauhan P 2009 *Mater. Charact.* **60** 1512
[5] Dikovska A O, Atanasova G B, Avdeev G V and Nedyalkov N N 2016 *Appl. Surf. Sci.* **374** 65
[6] Sondi I and Salopek-Sondi B 2004 *J. Colloid Interface Sci.* **275** 177
[7] Panáček A, Kvitek L, Prucek R, Kolář M, Večeřová R, Pizúrová N *et al J. Phys. Chem. B* **110** 16248
[8] Lyon D Y, Adams L K, Falkner J C and Alvarez P J 2006 *Env. Sci. Tech.* **40** 4360
[9] Kim Y H, Lee D K, Cha H G, Kim C W, Kang Y C and Kang Y S 2006 *J. Phys. Chem. B* **110** 24923
[10] Li P, Li J, Wu C, Wu Q and Li J 2005 *Nanotechnology* **16** 1912
[11] Du J and Gebicki J M 2004 *Int. J. Biochem. Cell Biol.* **36** 2334
[12] Saleh R and Djaja N F 2014 *Spect. Acta Part A: Mol. Bio. Spec.* **130** 581
[13] Al-Fwadi E, Al-Alias M F and Al-Shaikley F 2008 *J. Phys.* **5** 63
[14] Thirumavalavan S, Mani Y and Suresh S S 2015 *J. Nano- Electr. Phys.* **7** 04024
[15] Kaur J and Tripathi S K 2015 *Acta Meta. Sinica (English Letters)* **28** 591
[16] Dhillon G S, Brar S K, Kaur S and Verma M 2012 *Crit. Rev. Biotechnol.* **32** 49